

Historical Trend of Polycyclic Aromatic Hydrocarbons Contamination in Recent Dated Sediment Cores from The Imo River, Southeast Nigeria

Inyang O. Oyo-Ita , Orok E. Oyo-Ita

Abstract— The distribution and historical changes of polycyclic aromatic hydrocarbons (PAHs) contamination in recent sediment cores from the Imo River were evaluated over the last ca 5 decades. The concentrations of total PAHs (TPAHs-sum of parent and alkyl) ranging from 402.37 ng/g dry weight (dw) at the top layer of the Estuary site (ES6; 0-5 cm) to 92,388.59 ng/g dw at the near-top layer of the Afam site (AF5; 5-10 cm) indicated that PAHs contamination was localized not only between sites but also within the same cores. Sediment-depth profiles for the four (Afam-AF, Mangrove-MG, Estuary-ES and illegal Petroleum refinery-PT) cores generally revealed irregular TPAHs patterns, except the fact that the levels became maximized at the near-top layers (5-10 cm; ca.1997-2005). This time-frame coincided with the period of intensive oil bunkering/pipeline vandalism by the Niger Delta militant groups. The general decline in TPAHs levels up-cores to the most recent layers (0-5 cm) was attributed to the recent offer of amnesty to the Niger Delta militants and subsequent effort by the Nigerian government in clamping down the illegal activity of the economic saboteurs. Examination of perylene distributions down cores revealed natural terrestrial biogenic, pyrogenic and non-marine petrogenic origins for the compound at different sites. Thus, in view of the uncertainty surrounding the mechanism of perylene formation, the study highlighted the need for more attention to be paid to the involvement of terrigenous instead of aquatic OC in arriving at the probable mechanism for the compound.

Index Terms— Distribution, Historical trend, Imo River, Origin, Perylene..

I. INTRODUCTION

Polycyclic aromatic hydrocarbons (PAHs) have been listed as priority compounds due to their carcinogenicity, mutagenity, acute toxicity and persistency in the environment [1]. Reports by many researchers have shown that PAHs are ubiquitous compounds, found in all compartments of the environment and tend to adsorb to aquatic sediments ([2], [3]).

As time progresses, the deposition of contaminants led to the differences in the distribution of PAHs at different depth intervals. In other words, diverse distributions of

PAHs in different years are recorded in sediment due to differences in energy structure and economic development [4]. Therefore, it is very important to analyze sediment cores in order to understand the historical trends of PAHs deposition in the Imo river region. So far, the temporal historical trends of PAHs in sediment cores have been studied extensively around the world (e.g. [5],[4],[6]), and many of them show that the temporal trends corresponded to the vertical distributions in sediment cores. However, the knowledge of historical trends of PAHs sources in tropical African countries is relatively limited. To our knowledge, this is the first investigation on historical trends of PAHs contamination in the imo river sediments that reflects events that occurred after the first commercial discovery of crude oil in Nigeria in 1956.

Previous studies of the river sediment focused mainly on the surface sediment characterization ([3],[7],[8],[9]).

Radiometric methods have been shown to be reliable in a large number of dating studies of sediments, whether such sediment accumulation rates are uniform or non-uniform [10]. ^{210}Pb supply mechanisms are commonly assessed by three models, viz. Constant Flux Constant Sedimentation (CFCS), Constant Rate of Supply (CRS) and Constant Initial Concentration (CIC). The choice of CRS in the present investigation was based on the assumption that there is constant net rate of supply of ^{210}Pb from the water column to the sediment, irrespective of changes that may have occurred. The study combined radiometric and sedimentological investigations to assess sedimentation rates and the chronological succession of sediment layers that may be related to historical events.

Perylene, a 5-ring PAH has been extensively reported by many researchers in marine, lake, river and estuarine sediments to have diverse origins including non-marine oils [11]; natural gas combustion product ([12],[13]) *in situ* terrigenous and/or aquatic organic carbon (OC) production ([11],[14],[15]) and tropical termite mounds [16]. Thus, the origin of perylene has been a matter of continued debate as the mechanism of its formation still remains enigmatic.

The Imo River environment represents one of the few environments suitable for the investigation of the diverse origins of perylene with the view to having a better insight into the mechanism of perylene formation in the nearest future. This is because its environmental characteristics provide a veritable means of tracing both natural (terrestrial or aquatic) and anthropogenic

Inyang O. Oyo-Ita, Environmental/Petroleum Geochemistry Research Group, Department of Pure & Applied Chemistry, University of Calabar, Nigeria

Orok E. Oyo-Ita, Environmental/Petroleum Geochemistry Research Group, Department of Pure & Applied Chemistry, University of Calabar, Nigeria



(petrogenic or pyrogenic) origins for the compound. Therefore, the main objectives of the present study were to: (i) delineate the distribution of PAHs in sediment cores of the study area, (ii) determine the historical trends of PAHs contamination over the last ca. 5 decades and (iii) evaluate the diverse origins of perylene in a single sedimentary environment.

II. STUDY AREA

Details about the study area are described by [9]. Briefly, the Imo River is one of the tributaries of the southeastern Niger Delta, Nigeria (Fig. 1). It originates from the hill region of Imo State and flows through several towns, villages and farmland areas and empties directly into the Bight of Bonny, which then flows into the Atlantic Ocean. The river lies between 5° 55'N and 7° 1'E. It is shallow, with depth ranging from 1 to 10 m at flood tide and from less than 1 cm to ca. 8 m maximum at ebb tide. The study area belongs to the low lying coastal deltaic plain of SE Nigeria; the terrain is virtually flat or gently undulating, sloping generally towards the Atlantic [17]. Because of this, part of its watershed is generally flooded, especially during intensive rainfall. In March 2012, the Nigerian hydrological service announced an impending rise in water height to about 5 m occasioned by global climate change that subsequently caused devastating consequences to life and properties of coastal communities who ignored an early warning of evacuation from the region to the hinterland. The entire river appears cloudy (except at the congruence with other tributaries) as a result of high suspended sediment load due to rapid weathering. These suspended particles may raise the water temperature, reducing the oxygen content of the river water and limiting phytoplankton growth [9].

An important vegetation input to the river consists of floating grass on the shoreline (which often forms large floating mats) and mangrove. However, there are a few industries (e.g. the Afam power station and fertilizer plant) aligned near part of the riverbank and the prevalence of illegal oil refinery and bunkering activity, resulting in spillage.

Geologically, the study area belongs to the SE part of the Cretaceous and Tertiary sedimentary basin of the southern Niger Delta. The hydrogeology is related directly to the structural setting of the Benin Formation which is the aquiferous layer of groundwater supply. The layer consists of sand and gravel that are enhanced by hydraulic conductivity and transmissivity of the water-producing layer (aquifer) such that the water table is invariably at shallow depth. However, minor interaction with shale gives rise to a multi-aquifer system, two components of which were identified by [17]. The upper one (Holocene in age) is more prolific, extends to ca. 80 m and is mainly fine-grained sand. The other (Oligocene) is less prolific and is beneath this depth. These structural features provide channels for the flow and accumulation of ground water, which afford springs and seasonal streams [17].

III. EXPERIMENTAL METHODS

A. Materials

The following analytical grade solvents including dichloromethane, methanol, hexane, acetone, isooctane and ethyl acetate were provided by Dr. Ehrenstofer GmbH (Augsburg, Germany) and Merck (Hohenbrunn, Germany). Silica gel (0.063-0.200 mm), anhydrous sodium sulfate and aluminum oxide active neutral (0.063-0.200 mm) were also obtained from Merck. The vessels used for analysis were pre-cleaned with ethyl acetate followed by acetone and heated at 300 °C overnight.

B. Samples and Radiometric Analysis

The Imo River was divided into four different sites, each site made up of one sediment core of 30 cm long (designed to correspond to a dated time-scale of ca. 5 decades to coincide with the period of first commercial discovery of crude oil in Nigeria). Each core was cut into 6 sections of 5 cm interval.

Site I consists of samples obtained near thick mangrove vegetation stands (MG1-6) expected to contain dominant terrestrial organic carbon (OC); Site II consists of samples obtained near Afam Power Station (AF1-6) where natural gas combustion takes place; Site III consists of samples collected near illegal local petroleum refinery site (PT1-6) and Site IV consists of samples collected near the estuary (ES1-6) where commercial fishery activity takes place. All cores were collected in 12th August 2013 after the devastating flood episode of 2012 using a calibrated PVC corer, wrapped with pre-cleaned aluminum foil, kept in a cooler containing ice, brought to the laboratory and stored at -20 °C in a deep freeze until further processing.

Due to tidal influx and mixing arising from sediment re-suspension, core collected towards the estuary site (ES) was not well preserved. Thus, radiometric analysis for the ES core was not possible. Samples from individual layers were dried at 60 °C for 3 days and then weighed to estimate dry bulk density and cumulative mass depth. The dried samples were homogenized with a pestle and mortar before conditioning and analysis [10]. Samples were analyzed using direct γ assay (Ortec HPGe GWL series well-type) housed in a 10 cm Pb shielding with Cu, Cd and plastic lining, operated under Canberra Genie 2000 software. For Gamma counting, the samples were put into polystyrene tubes. Excess ^{210}Pb ($^{210}\text{Pbxs}$) was determined by subtracting the specific activity of ^{214}Pb (i.e. ^{226}Ra) from the total ^{210}Pb specific activity. This calculation was based on the assumption that the intermediate daughter product, ^{222}Rn , is in equilibrium with ^{226}Ra . The samples were then sealed and left for three weeks to allow equilibrium to be reached before gamma counts were carried out.

Radiometric measurements were performed in a very low background P-type germanium well detector (Canberra Industries), which offered a relative efficiency of 40% and a 4π counting geometry. The counting device was placed in a low-level background laboratory, in order to ensure a very low detection threshold for environmental radioactivity. Such a precaution was particularly necessary for the isotopes of interest here (^{210}Pb and ^{214}Pb). Details of the method are given in Appleby et al. 1992 [18]. This

analytical process allowed us to measure ^{210}Pb isotope with detection limits of below 6mBq/g. The experimental error for this measurement, taking into account the different sources of error due to the sampling and analytical procedures, was approximately $\pm 25\%$. Counts were carried out on individual samples for time periods ranging from 10^5 to 3×10^5 s. For every 10 samples analyzed, the background level was measured over periods of 2×10^5 to 3×10^5 s. Sample specific activity A, and total uncertainties of calculated specific activity values, $\%A$, were expressed in Becquerel per kilogram of dry weight (Bq/kgdrywt). The standard deviation expressed the 95% confidence level [10].

C. Grain Size, Bulk Density, TOC and TN Determinations

Sediment grain sizes were analyzed using a laser particle sizer (LS 200, Beckmann-Coulter) with a mesh range of 0.375-1000 μm . A detailed description of these analytical techniques is given in Strauss et al. (2015)[19].

Bulk density (BD) measurements were performed by determining the volume of frozen samples with the Archimedes Principle that involved quantifying the water displaced in a water-filled glass beaker using a balance (FCB 8K0.1, Kern; [10]. BD was calculated using the following equation:

$$\text{BD} [10^3 \text{ kgm}^{-3}] = \frac{\text{sample dry weight} [10^3 \text{ kg}]}{\text{sample volume} [\text{m}^3]}$$

Freeze-dried samples were de-carbonated in 85% syrupy orthophosphoric acid in several stages until bubbling stopped and rinsed in de-ionised water until neutral pH. The determination of total organic carbon (TOC) and total nitrogen (TN) contents was performed by flash combustion at 1024°C, followed by thermic conductivity detection in triplicate in a CHNS Elemental Analyser, Carlo Erbar 1108.

D. Extraction and Clean-up

Prior to extraction protocol, sediment samples were "spiked" with the perdeuterated surrogates (naphthalene- d_8 , anthracene- d_{10} , pyrene- d_{10} , benzo[a]pyrene- d_{12} , benz[a]anthracene- d_{12} and triphenylamine (TPhA) as internal standard. Samples (1g each) were extracted three times by sonication (ultrasons 9L; 360 W average power output and mean operating frequency of 40 KHz) for 30 min with 15 ml of solvent mixture (acetone/hexane; 1:1 v/v). After centrifugation at 3500 rpm for 10 min, the clear supernatants were removed and the combined extract was concentrated to near-dryness under a stream of pure nitrogen and re-dissolved in ~0.5 ml hexane prior to clean-up.

Cleanup was performed by adsorption chromatography in an open glass column packed with 1 g anhydrous sodium sulfate (top), 2 g neutral alumina (middle; activated at 400 °C, 5% water deactivated) and glass wool (bottom). The eluent was concentrated to an accurate 300 μL by a gentle stream of N_2 gas and preserved in a dark-brown vial prior to gas chromatography-mass spectrometry (GC-MS) injection.

E. Instrumental Analysis And Quality Assurance/Control

Analysis of the aromatic fractions was accomplished with a TRACE GC-MS Thermo-Finnigan (Manchester, UK) in the electron impact (EI) mode at 70 eV. A 30-m, 0.25-mm-inner diameter capillary column coated with 0.25 μm of ZB-5MS stationary phase (Phenomenex Zebron; USA) was used. The carrier gas was helium with a constant flow rate of 1.2 ml/min. The injector temperature, in "splitless" mode, was held at 280 °C and the purge valve was activated 50 s after the injection. Column temperature was held at 60 °C for 1 min, then the temperature was increased to 200 °C at 10 °C/min and finally to 320 °C at 4.8 °C/min, holding that temperature for 10 min. Transfer line and ion source temperatures were held at 250 °C and 200 °C, respectively. Data were acquired in the SIM mode with 6 min of solvent delay and processed by the X-calibur Thermo Finnigan software (San Jose, California, USA).

One analytical blank was run with every batch of 2-5 samples to check background contamination during the extraction and purification steps. To remove background contamination, we corrected PAHs concentrations by subtracting the mean of the analytical blanks from the concentrations of PAHs. Deuterated analogues were used for both recovery and quantification corrections. The analysis of the samples was repeated in triplicate and relative standard deviations were calculated. Limits of detection (LOD) and limits of quantification (LOQ) were estimated as the average signal of the blanks plus three times the standard deviation of the signal of the blanks and average signal of the blanks plus ten times the standard deviation of the signal of the blanks, respectively.

The parent and alkyl PAHs in the samples were identified on the basis of retention time and ion fragment profile compared against authentic standards, whereas quantification was conducted using multipoint internal calibration method. A calibration curve (detector response versus amounts injected) was performed for each compound to be quantified. The linear range of the detector was estimated from the curve generated by plotting detector signal versus amount injected. All measurements were performed in the linear ranges for each target compound. In few cases, the samples were re-diluted and re-injected for fitting within the linear range of the instrument.

IV. RESULTS AND DISCUSSION

A. Sediment Characteristics

The accuracy and reproducibility of the PAH analytical method were satisfactory. The percentage recoveries of the 16 priority listed PAHs and others including the alkylated homologs ranged from 60% to 130% except naphthalene which had only 40% recovery. The relative standard deviations of three replicates were less than 20% except naphthalene (23%). These results were comparable with those reported by previous workers such as Zheng et al. (2002)[20] and Ke et al. (2005)[5], and also fulfilled the acceptance criteria suggested by [21], suggesting that the analytical procedures were subjected to quality assurance and quality control.

The cores were dominated by gray-dark sandy silt and a minor clay deposits at depths 5-30 cm, whereas a relatively higher silt/clay fraction were deposited at the top layers (0-5 cm). The fairly constant bulk density values recorded for the lower layers (Table 1) suggested occurrence of a steady sedimentation rates at the three coring sites. However, the slight decline in bulk density values at the top layers (0-5 cm) was associated with the flood episode of 2012, leading to a slight change in the sedimentation rates at the top layers. In other words, except for the top layers, no periods of surface mixing were observed in the vertical structure of the dated sediments and generally had a well-defined depositional chronology.

The cores were dated by the application of ^{210}Pb -derived model. The $^{210}\text{Pb}_{\text{xs}}$ specific activity profile was relatively homogeneous for depths 5-30cm (3.06-3.24 Bq/kg) and differed at 0-5 cm (4.24-4.35 Bq/kg; Table 1). The depths at which $^{210}\text{Pb}_{\text{xs}}$ specific activities were homogenous coincided with the depths 5-30 cm and differed from depth 0-5 cm in which therelatively higher silt/clay content and slight decrease in bulk density occurred (Table 1).Consequently, the sediment deposits scenario did not meet the conditions for applying the CFCS model [10].Therefore, CFCS could not be used to calculate mean sedimentation rates for the cores. An alternative way to analyze such a profile was to assume that there is a constant net rate of supply of ^{210}Pb from the water column to the sediment, irrespective of changes that may have occurred in the net dry mass sedimentation rate[22].Therefore, calculated ages based on CRS model assumed the constant sedimentation rates for the whole cores. These sedimentation rates were derived from the mean slope of ^{210}Pb specific activity plotted on a logarithmic scale. Mean sedimentation rates for AF, PT and MG cores were ca. 0.60, 0.58 and 0.62 cm/yr, respectively, with an overall mean of ca. 0.60 ± 0.07 cm/yr. This mean value was subsequently used for assessing the historical trends of contamination by PAHs for the river sediment.

Ages of specific layers were determined by dividing their depths by the corresponding sedimentation rates.Age resolution of the cores represents an average provisional record of ca. 50 yr. of sedimentation history.Sedimentary records for the river date from ca. 1964 (ca. 8 yr after the first commercial discovery of oil in Nigeria in 1956) to ca. 2013 (ca. 4 yr after an amnesty offer to Niger Delta militant groups by the Nigerian government in 2009).

Total organic carbon (TOC) profiles down cores exhibited low values that ranged from 0.10% at the middle layer (PT3; 15-20 cm) of the PT to 1.02% at near-top layer (AF5; 5-10 cm) of the AF site. These low TOC values may be a result of poor adsorbability of the OC on the negatively charge solid matrix (quartz in nature), shallow water depth, low primary productivity and the characteristic sheltered basin morphology predominated by sand fraction [9]. On the other hand, the total nitrogen (TN) contents did not vary widely with depth and generally exhibited values <0.05 , indicating a relatively constant and minimal aquatic flora production

down cores [23]. To support the low contribution of aquatic flora relative to terrestrial OM input, atomic C/N values for the four cores were calculated and the values ranged from 18.9 at the near-bottom layer (AF3, 20-25 cm) of AF to 35.3 at the top layer of MG core (MG 6, 0-5 cm; Table 1). Oyo-Ita and Oyo-Ita, (2012)[3] reported a similar high C/N value for the top layer of Ukwa Ibom lake sediment, SE Nigeria and attributed the elevated level to greater wash-in of land-derived OM following pave-road extension exercise that involved tree logging/forest clearing. The elevated C/N scenario at the top layers here most likely reflected the effect of flood associated with the recent intense rainfall occasioned by global climate change, carrying larger amounts of land-derived debris to the river.

It is a common knowledge that properties of sediment such as TOC would influence the distribution and concentrations of PAHs and other hydrophobic organic compounds (Ke et al. 2005). In the study, a good correlation existed between TOC contents and TPAH concentrations for the ES ($r^2 = 0.5663$). However, poor correlations existed for the PT ($r^2 = 0.0063$), AF ($r^2 = 0.2113$) and MG ($r^2 = 0.1069$) cores (Fig. 2 a, b, c,d). This means that some local contamination sources might have interfered in the linear relationship between the PAHs and OC contents in the study area. Therefore, PAH concentrations were normalized by the respective OC contents to eliminate variations generated by the inherent property of the sediments such as OC.

B. Spatial and Vertical Distribution of PAHs in Estuary and Afam Cores.

Generally, the spatial variation in PAHs concentrations in the 6 layers of the four cores might be ascribed to differences in hydrodynamic regimes related to the present and past river discharges and tidal influx, changes in sediment particle size characteristics in the individual cores and non-homogenous inputs from point- and non-point-sources of PAHs in the region [24].

The PAHs distribution by number of rings for the top layer of AF core was as follows: 2->3->4->5->6-rings characteristic of dominant input from oil, while a 2->5->4->3->6-rings trend was found for the ES core, indicative of a mixed source scenario with an enhanced pyrogenic source inputs (Fig. 3 a, b). It is a well-established knowledge that higher proportions of alkyl PAH analogs are often found in petroleum than in pyrogenic sources [25]. In support of the oil dominance, Fig. 4 a shows relatively higher abundance of alkyl PAHs (350.13 ng/g dry weight-dw) in the AF than the ES core (181.86 ng/g dw).

The vertical distributions of TPAH for the AF and ES cores are shown in Fig. 5 a. In all depth intervals, the AF exhibited significantly higher TPAH levels than the ES except at the middle layer (15-20 cm). The relatively higher clay fraction (22.1%) and TOC content (0.94%) in the middle layer of ES (ES3) facilitated the adsorption and accumulation of PAHs, and may partly account for the relatively high level (615.29 ng/g dw) in the layer relative to AF3 (422.15 ng/g dw). The TPAH level measured at AF5 (5 – 10 cm) was about 5 order of magnitude higher than those measured in other layers of

the AF core. Field observation revealed that there was a smell of oil in the AF5 sample but not in others of the AF core, suggesting that oil contamination at the AF5 was accidental, and did not permeate significantly down core.

An increase in TPAH levels from top layer (0 – 5 cm) to the middle (15 - 20 cm) and then declined thereafter to the bottom layer (25 – 30 cm) was found for the ES core. The differences in TPAHs levels between sediment layers of the ES core were not significant according to one way ANOVA test ($F = 3.56$; $p = 0.088$), implying that depth did not have significant effect on the distribution of TPAH at the ES site.

The distribution of individual PAHs in both AF and ES cores are complex and did not follow any regular pattern (Table 2). An *insitu* degradation or metabolism by benthic communities could have contributed to the dispersion profile. Nevertheless at the layer 5-10 cm (AF5), the low molecular weight (LMW) PAHs including naphthalene, acenaphthene, acenaphthylene, anthracene and phenanthrene were the dominant compounds (concentrations exceeding 1,000 ng/g dw), supporting the accidental oil discharge scenario to the sediment layer.

Besides the observed dispersion, there was no significant difference in the concentrations of individual PAHs in all layers of the ES core. Although the concentrations of naphthalene were pervasively high in all layers of ES, higher proportion of high molecular weight (HMW) PAHs was apparent. The higher percentage of HMW to total PAHs calculated for the ES relative to the AF core (Fig. 6) supported the higher pyrogenic contribution to the ES relative to the AF over the last ca. 5 decades. The implication here is that the two sites were influenced predominantly by PAHs of different sources. Therefore, localization of the input sources played an important role in PAH contamination for the two sites. In addition, the percentage HMW to TPAH values did not vary significantly with depth for the two cores except at the AF5 (5- 10 cm), suggesting that the sources of contamination were fairly constant over the last 5 decades.

C. Spatial and Vertical Distribution of PAHs in Mangrove and Illegal Petroleum Refinery Cores

Comparing top layers data between the MG and PT cores, the following distribution trends were found for PAHs according to number of rings: 2->3->4->5->6-rings and 2->3->5->4->6-rings, respectively (Fig. 3 c, d). The prevalence of 2- and 3- ring types is indicative of predominance of petrogenic over pyrogenic source input to the two sites, with higher proportion of fossil fuel combustion influence at the PT relative to the MG site as evidenced in the higher proportion of % HMW to TPAH (Fig. 6 b). There were no consistent trends in the vertical distributions of PAHs according to ring size for the two sites. However, it appears that the 2- and 3-ring types' levels remained highest at 5-10 cm for the two cores, indicating that similar anthropogenic pressure occurred during the period ca. 1997-2005 of sediment deposition (Fig 3 c, d). Comparing the levels of alkyl PAHs between the two cores, it is apparent that the extent of impart by oil was higher in the PT (502.64 ng/g dw) than MG site (67.76 ng/g dw; Fig 4 b).

The vertical distributions of TPAHs in the MG and PT cores are shown in Fig. 5 b. In all layers, the PT exhibited significantly higher TPAH concentrations than the MG except at MG1 (25-30 cm) and MG4 (10-15 cm) where a reverse trend occurred. The distributions of TPAH down cores for the two cores did not follow any regular trend except that the levels peaked at the near-top layers (5 – 10 cm) and became minimized at the bottom layers (25-30 cm). In the two cores, depth had no significant effect on the vertical distribution of the TPAHs (one way ANOVA test; $F = 3.4$; $p = 0.09$). The value was less than the critical F value of 4.96, implying that the levels of TPAHs in all layers did not vary widely over the last ca. 5 decades of sediment deposition.

The concentrations of individual PAHs in the two cores were also complex and did not reflect any regular pattern (Table 3). Nevertheless, the only observable trends were found in naphthalene (in the case of the MG) and acenaphthene (in the case of the PT) which remained pervasively dominant in all layers. Differences in *insitu* degradation by microbes or metabolism by benthic communities between the two cores may account for the dispersion found for most of the individual PAHs. The non-uniformity in the vertical distribution of percentage of HMW to TPAHs for the two cores confirms that petroleum residue was not the exclusive source of PAHs contamination (Fig. 6 b), but that pyrogenic input arising from combustion of fossil fuel associated with the illegal oil refining process must also be involved. The result therefore confirms that localized contamination was not only evidenced between the two cores but also within the same cores.

D. Historical Trends of PAHs Contamination

The historical trends of normalized PAH distribution down cores are shown in Fig. 7 and indicates that the contamination was heaviest in the near-top layers (5-10 cm) for the three dated cores (AF, MG and PT). The heavily impacted layer according to the estimate corresponded to the period ca. 1997-2005. In other words, PAH contamination of the river was very serious in the mid-1990s and 2000s. This time-frame coincided with the period of intensive oil bunkering/pipeline vandalism activity by the Niger Delta militant groups. In June, 1998, a 16-inch underground Shell pipeline burst, discharging about 800,000 barrels of oil into the area [26]. Oil companies including Shell Petroleum Development Company operating in Nigeria often blame oil spills on armed militants operating in the Niger Delta, who campaign for a fairer allocation of oil revenue to locale in the oil-rich region. The contamination then dropped to the most recent period (ca. 2005-2013, 0-5 cm). Although the decline in PAHs contamination was more significant in the AF core, the scenario was linked to the recent offer of amnesty in 2009 and subsequent clamped down on vandals/militants by the joined armed forces empowered by the Nigerian government.

After the first commercial discovery of petroleum in Nigeria in 1956, sediment cores from the MG, ES and PT sites except the AF exhibited gradual and steady increase up-cores in PAH contamination from early 1960s to mid-1990s. The increase may be associated with

increasing urbanization and economic development in the region. The slight decline up-core in all cores except AF signifies that despite the concerted effort by the Nigerian government to curb the activity of the economic saboteurs, some pockets of bunkering activity and illegal oil refineries still persisted going by the recent report accredited to the Minister of Petroleum in 2015.

In the case of the AF core, the pattern differed slightly, showing a relatively higher TPAH level in the bottom layer (25-30 cm; ca. 1964 -1972). The plausible explanation for the variation in the AF was thought to be the effect of construction of the Afam power station complex in the early 1960s (when utilization of natural gas and petroleum condensate for power generation was at its peak). In addition, Eyama-Elleme, a village near the AF area experienced an oil spill in the late 1960s caused by a fire explosion in which a vast area was buried under a hard-rock crust of burnt oil many feet thick [26], contributing to the enhanced impact in the bottom layer.

E. Origins of Perylene

The study was able to identify in a single environment three different origins for perylene by examination of its distribution patterns. Perylene has not only been reported by many researchers to be produced by *insitudiogenesis* of biogenic precursors of terrestrial OC origin (eg. [11],[14]) and aquatic origin ([27],[28]), it has also been shown to be derived from anthropogenic sources ([12], [15]).

In the study, among the four top layer samples, perylene levels were most concentrated in the ES site which was within 3 orders of magnitude higher than those in other sites. The relatively high perylene level (54.43 ng/g dw; Table 2) at the site where commercial fishery activity takes place may be associated with input from liquid fossil fuel combustion process arising from boat traffic/vehicular exhaust emission. The deduction is supported by the relatively higher proportion of percentage HMW to TPAH (characteristic of pyrogenic input; Fig. 8) for the site.

Furthermore, a comparison of vertical distribution profiles of perylene between AF and relatively pristine MG revealed different origins for the compound (Fig. 9). For instance, a uniform perylene distribution trend observed for the MG down core indicated a constant production over the last ca. 5 decades, most likely reflecting a diagenetic origin [24]. Result of atomic C/N calculation (> 15) revealed that the Imo River sediment is dominated by terrestrial (land-derived) OC, and lesser amounts of aquatic (e.g. micro-algae/phytoplankton) production (Table 1; [29], [30], [31]). Therefore, the proposed biogenic production for perylene in the MG was rather linked to diagenesis of terrigenous OC instead of an aquatic origin.

In the case of the more contaminated AF site, an irregular perylene distribution trend down core that maximized (734.53 ng/g dw) at 5-10 cm layer (AF5; 1997-2005, a period when accidental discharge of oil was earlier reported to have occurred) was found. Since the Nigerian oil/gas is believed to be predominantly derived from terrestrial OC on the basis of detection of oleanane, perylene occurrence in the AF site can thus be linked to a

non-marine oil origin. Hence, the Imo River environment truly represents one of the few environments suitable for the investigation of the diverse origins of perylene. We therefore recommend that concerted research effort should be directed more towards utilization of terrigenous instead of aquatic OC in understanding the mechanism of perylene formation.

V. CONCLUSIONS

The Imo River environment provides a veritable means of tracing the diverse origins of perylene as well as assessing the historical trends of PAHs contamination after the first commercial discovery of oil in Nigeria in 1956. The vertical distributions of perylene in the MG revealed a constant trend that suggests natural biogenic origin derived from terrigenous OC. While pyrogenic origin for the compound was established for the ES, the AF exhibited a profile consistent with a non-marine petrogenic source. Hence, in view of the uncertainty surrounding the probable mechanism of peryleneformation, we recommend that concerted research effort should be focused more on the involvement of terrigenous instead of aquatic OC.

No regular trends were found in the distribution of TPAHs in all cores, except that the parameter peaked at the near-top layers corresponding to the period of intensive oil bunkering/pipeline vandalism and illegal oil refining activity. A general decline thereafter up-core was most likely attributable to the recent offer of amnesty and subsequent effort by the Nigerian government in clamping down the illegal activity of the Niger Delta militant groups.

VI. ACKNOWLEDGEMENTS

We are sincerely thankful to the European Association of Organic Geochemists (EAOG) for the financial support that made this research work possible. We are also grateful for the excellent scientific equipment provided by the Institute of Environmental Assessment and Water Research, Spanish Council of Scientific Research (CSIC), Barcelona, Spain and ADECYTE at little or no cost.

REFERENCES

- Christensen ER, Arora S (2007). Source apportionment of PAHs in sediments using factor analysis by time records: application to Lake Michigan, USA. *Water Res.* 23: 1 -8.
- [2]Liu Z, Zhang H, Tao M, Yang S, Wang L, Liu Y, Ma D, Zhiming H (2007). Organochlorine pesticides in consumer fish and mollusk of Liaoning province, China: distribution and human exposure implication. *Arch. Environ. Contam. Toxicol.* 59: 444-453.
- [3]Oyo-Ita OE, Oyo-Ita IO (2012). PAHs depositional history in recent core sediments from Ukwabom lake, SENigeria. *Environ. Geochem. Health* 35: 189 – 199.
- [4]Guo J-y, Wu FC, Luo XJ, Liang Z, Liao HQ, Zhang RY (2010). Anthropogenic input of polycyclic aromatic hydrocarbons into five lakes in western china. *Environ.Pollut.* 158(6): 2175-2180.
- [5]Ke L, Yu H, Wong S, Tam Y (2005). Spatial and vertical distribution of polyaromatic hydrocarbons inMangrove sediments. *Sci. Tot. Environ.* 340: 177-187.

- [6] Zhang R, Zhang F, Zhang T (2013). Sedimentary records of PAHs in a sediment core from tidal flat Haizhou Bay, China. *Sci. Tot. Environ.* 450:280-288.
- [7] Sojino S, Wang J, Sonibare O, Zeng E (2010). Polycyclic aromatic hydrocarbons in Sediments and soils from oil exploration areas of the Niger Delta, Nigeria. *Hazard. Mater.* 174: 641- 647.
- [8] Ekpo BO, Ebirien PF, Okon DE, Hab LM (2012). Distributions of Fossil Fuel Biomarkers in Sediments as Proxies for Petroleum Contamination of Coastal Environment of the Niger Delta, Southeastern Nigeria. *J. Appl. Sci. Environ. Sanit.* 7(2): 75-86.
- [9] Oyo-ita OE, Oyo-Ita IO (2013). Fatty acids and alcohols distributions and sources in surface sediments of the Imo River, SE. Niger Delta, Nigeria. *Environ. Natl. Reso. Res.* 2: 101 -113.
- [10] Arnaud F, Magand O, Chapron E, Bertrand, Boe's, X, Charlet, MA, Me'lie`res, F (2006). Radionuclide dating (²¹⁰Pb, ¹³⁷Cs, ²⁴¹Am) of recent lake sediments in a highly active geodynamic setting (Lakes Puyehue and Calma-Chilean Lake District). *Sci. Tot. Environ.* 366: 837-850.
- [12] Grice K, Lu H, Atahan P, Asif M, Hallmann C, Greenwood P, Maslen E, Tulipani S, Williford K, Dodson J (2009). New insights to the origin of perylene in geological samples. *Geochim. Cosmochim. Acta* 73: 6531 -6543.
- [13] Bixtong Y, Zhuhuan Z, Ring M (2006). Pollution source identification of polycyclic aromatic hydrocarbons of soils in Tianjin area, China. *Chemos.* 64: 525-534.
- [14] Oyo-Ita OE, Offem JO, Ekpo BO, Adie P (2013). Anthropogenic PAHs in Mangrove sediments of the Calabar River, S.E. Niger Delta, Nigeria. *Appl. Geochem.* 28: 212 -219.
- [15] Ekpo BO, Oyo-Ita OE, Oros DH, Simoneit BRT (2011). Distribution and sources of polycyclic aromatic hydrocarbons in surface sediments from Cross River estuary, S. E. Niger Delta, Nigeria. *Environ. Monitor. Assess.* 34: 225-237.
- [16] Marynowski L, Kurkiewicz S, Rakocinski M, Simoneit BRT (2011) Effects of weathering on organic matter: 1. Changes in molecular composition of extractable organic compounds by paleoweathering of a lower carboniferous (Tournaisian) marine black shale. *Chem. Geol.* 285: 144-156.
- [17] Wilcke W, Amelung W, Krauss M, Martins C, Bandeir RA, Gracia M (2003). Polycyclic aromatic hydrocarbons (PAHs) patterns in climatically different ecological zones of Brazil. *Org. Geochem.* 34: 1405 - 1418.
- [18] Ezeayim V, Okereke CA (1996). The effects of petroleum activities in Nigerian soil environment. *Glob. J. Pure Appl. Sci.* 11: 285-297.
- [19] Appleby PG, Richardson N, Noland PJ (1992). Self-absorption corrections for well-type Germanium detectors. *Nucl. Inst. Meth.* 371: 228-233.
- [20] Strauss J, Schirrmeister L, Mangelsdorf K, Eichhorn L, Wetterich S, Herzsuh' U (2015). Organic-matter quality of deep permafrost carbon - a study from Arctic Siberia. *Biogeosci.* 12: 2227-2245.
- [21] Zheng G, Man B, Lam M, Lam P (2002). Distribution and sources of polycyclic aromatic hydrocarbons in the sediment of a sub-tropical coastal wetland. *Water Res.* 36: 1457 - 1468.
- [22] Burns W, Mankiewicz P, Bence A, Page D, Parker K (2007). A principal component and least squares method for allocating polycyclic aromatic hydrocarbons in sediment to multiple sources. *Environ. Toxicol. Chem.* 8: 1119-1131.
- [23] Appleby PG, Oldfield F (1992). In: Ivanovich, M., Haiman, R. S., (ed). Application of lead-210 to sedimentation studies. Oxford 7 Uranium series disequilibrium.
- [24] Gonzales-Vila FJ, Polvillo O, Boski T, Moura D, Andres de JR (2003). Biomarker patterns in a time-resolved Holocene/terminal Pleistocene Sedimentary Sequence from the Gurdiana River estuarine area (SW Portugal/Spain Border). *Org. Geochem.* 34: 1601-1613.
- [25] Dominguez C, Sarkar S, Bhattacharya M, Chatterjee B, Bhattacharya B, Jover E, Albaiges J, Bayona J, Alam MD, Satpathy K (2010). Quantification and source identification of polycyclic aromatic hydrocarbons in core sediments from Sundarban mangrove wetland, India. *Arch. Environ. Contam. Toxicol.* 59: 49-61.
- [26] Walker SE, Dickhut RM, Chisholm-Brause C, Sylva S, Reddy CM (2006). Molecular and isotopic identification of PAH sources in a highly industrialized urban estuary. *Org. Geochem.* 36: 619-632.
- [27] Okpo OC, Eze RC (2012). Vandalization of oil pipeline in The Niger Delta region in Nigeria and poverty: and overview. *J. Stud. Sociol. Sci.* 3(2): 13 - 21.
- [28] Wakeham SC, Farrington JN, Volkman JK (1981) Fatty acids, wax ester, triacylglycerols and alkyldiacylglycerols associated with particles collected in sediment traps in the Peru upwelling. *Advances Org. Geochem.* 18: 185-197.
- [29] Unlu S, Alpa B (2006). Distribution and sources of hydrocarbons in surface sediments of Gemlik Bay (Marmara Sea, Turkey). *Chemos.* 64: 764 - 777.
- [30] Meyers PA, Ishiwatari P (1998). The early diagenesis of organic matter in lacustrine sediments. *Org. Geochem.* 22: 185-200.
- [31] Ekweozor C.M, Telnaes N (1990). Oleanane parameter: verification by quantitative study of the biomarker occurrence in sediment of the Niger Delta. *Org. Geochem.* 16: 401-413.
- [32] Oyo-Ita IO, Oyo-Ita OE, Dosunmu MI., Dominguez C, Bayona JM, Albaiges J, (2016). Sources and distribution of petroleum hydrocarbons in recent sediment of the Imo River, SE Nigeria. *Arch. Environ. Contam. Toxicol.* 70: 372-382.

**Historical Trend of Polycyclic Aromatic Hydrocarbons Contamination in Recent Dated Sediment Cores
from The Imo River, Southeast Nigeria**

Table 1: Distribution profiles of the core sediment bulk characteristics at four sampling sites of the Imo River

Site(MSR -cm/yr)	SC	SA (Bq/kg)	BD (g/cm ³)	SBD (cm)	Coordinate	Period (Yr)	Age (Yr)	C/N	Grain size		
									Sand	Silt	Clay
Afam (0.60)	AF1	3.12	2.01	25-30	04 ⁰ 51.539' N 007 ⁰ 09.165' E	1964-1972	50	19.3	59.32	28.0	11.06
	AF2	3.07	2.21	20-25		1972-1981	42	19.6	72.84	20.1	7.03
	AF3	3.17	2.11	15-20		1981-1989	33	18.9	69.11	26.6	10.20
	AF4	3.16	2.15	10-15		1989-1997	25	20.6	64.44	28.1	7.45
	AF5	3.23	2.12	5-10		1997-2005	17	26.4	58.23	27.1	14.6
	AF6	4.24	1.59	0-5		2005-2013	8	32.7	37.66	45.1	17.18
Estuary (--)	ES1	-	-	25-30	04 ⁰ 52.654' N 007 ⁰ 09.251' E	-	-	20.4	50.77	31.0	18.22
	ES2	-	-	20-25		-	-	19.9	51.11	36.6	12.27
	ES3	-	-	15-20		-	-	21.8	52.78	27.0	22.16
	ES4	-	-	10-15		-	-	21.2	56.26	25.6	15.06
	ES5	-	-	5-10		-	-	23.7	63.01	28.3	8.61
	ES6	-	-	0-5		-	-	30.5	43.08	47.7	9.21
Petroleum (0.58)	PT1	3.11	2.04	25-30	04 ⁰ 53.056' N 007 ⁰ 09.261' E	1964-1972	50	19.5	62.86	27.6	9.52
	PT2	3.06	2.21	20-25		1972-1981	42	21.9	68.05	24.2	7.71
	PT3	3.17	2.11	15-20		1981-1989	33	19.2	65.01	23.6	11.32
	PT4	3.21	2.23	10-15		1989-1997	25	20.5	61.42	26.5	12.01
	PT5	3.19	2.21	5-10		1997-2005	17	22.3	69.31	22.6	8.05
	PT6	4.31	1.56	0-5		2005-2013	8	34.4	34.86	51.6	14.53
Mangrove (0.62)	MG1	3.11	2.15	25-30	04 ⁰ 53.167' N 007 ⁰ 08.823' E	1964-1972	50	21.5	63.25	30.7	6.05
	MG2	3.23	2.21	20-25		1972-1981	42	22.6	56.11	33.6	10.20
	MG3	3.16	2.11	15-20		1981-1989	33	19.5	59.88	31.0	9.10
	MG4	3.14	2.07	10-15		1989-1997	25	20.6	63.26	23.4	13.33
	MG5	3.21	2.23	5-10		1997-2005	17	21.7	69.06	22.1	8.80
	MG6	4.35	1.53	0-5		2005-2013	8	35.3	36.02	53.7	10.25

N/B: MSR= Mean sedimentary rate, SA=²¹⁰Pb_{xs} specific activity, SC=Sample code, BD=Bulk density, SBD=Sub-bottom depth.

Table 2: Concentrations (ng/g) of individual PAHs in sediment cores from the Afam and Estuary sites.

PAH	AF1	AF2	AF3	AF4	AF5	AF6	ES1	ES2	ES3	ES4	ES5	ES6
Nap	232.77	250.51	271.34	342.76	44952.83	684.12	64.84	73.89	123.86	100.7949	60.69143	89.42684
ACNthyl	6.50	3.98	5.08	13.73	6009.82	52.75	3.84	3.32	8.11	9.187501	8.16009	3.660797
ACNthene	5.71	0.49	0.46	5.58	2099.23	2.58	1.86	2.19	15.96	0.329761	4.082859	2.796727
Fl	7.40	3.15	3.22	8.44	2573.31	50.11	4.90	5.11	11.82	3.071417	6.86165	5.953219
Phe	21.90	4.45	4.14	17.72	1866.88	36.15	11.13	15.70	18.81	18.40612	12.50107	12.32131
Ant	9.83	12.07	17.66	9.743	587.78	15.73	5.22	5.03	8.71	18.44664	5.785101	5.386153
Flu	14.68	7.15	6.16	16.23	250.01	15.13	8.45	15.44	17.49	8.977216	10.51765	8.167452
Pyr	22.09	18.90	25.03	38.78	236.85	29.42	9.51	17.53	20.89	21.31463	16.96174	9.40439
B[a]A	9.76	10.09	9.84	10.86	978.02	13.34	10.96	14.10	11.74	10.31033	9.950107	9.803669
Chry	22.81	9.62	9.56	26.77	239.54	26.83	11.62	14.99	20.78	18.15355	17.5426	13.26205
B[b]F	10.50	9.27	8.64	8.20	94.34	17.80	8.23	8.57	11.33	14.25702	10.67404	9.351811
B[k]F	10.87	9.43	8.33	8.44	94.25	17.88	8.43	8.94	11.47	14.44633	10.68877	9.580744
B[a]P	61.64	3.08	3.14	11.79	69.44	4.59	5.24	11.33	10.55	7.022766	7.441183	6.604868
Pery	8.02	18.31	9.33	9.24	734.53	9.85	3.95	5.18	7.67	7.31758	4.914211	54.43112
InPy	15.65	10.32	11.89	16.48	827.71	21.09	11.87	16.03	15.82	13.70982	13.56652	12.02996
B[ghi]P	3.89	3.15	3.17	13.85	1023.43	22.41	7.06	16.44	18.81	9.333769	10.35219	7.175363
DB[a,h]A	2.17	1.29	1.08	1.36	158.96	15.66	2.84	6.58	21.43	18.43514	12.60037	5.729348
C1 Nap	5.15	7.54	4.112	4.20	2071.823	14.55	3.35	2.75	4.44	4.362363	4.111359	4.048646
C2 Nap	3.64	0.49	-0.02	4.12	2209.65	51.21	3.45	1.58	2.72	5.202373	4.842668	3.529657
C1 Phe	23.03	4.78	4.02	21.74	2448.84	30.62	10.08	12.84	25.04	24.35069	16.54659	12.4127
C1 Pyr	183.53	2.71	2.35	11.95	40.57	14.33	4.04	5.40	21.59	9.338841	18.85323	8.773338
Ret	7.50	1.64	-	4.93	8.89	3.11	2.10	2.12	-	0	3.813373	0

**Historical Trend of Polycyclic Aromatic Hydrocarbons Contamination in Recent Dated Sediment Cores
from The Imo River, Southeast Nigeria**

Table 3: Concentrations (ng/g) of Individual PAHs in Mangrove and illegal Petroleum refinery sediment cores

PAH	MG1	MG2	MG3	MG4	MG5	MG6	PT1	PT2	PT3	PT4	PT5	PT6
Nap	58.66	101.90	83.74	102.43	133.04	93.82	59.06	173.74	85.72	58.72915	762.9725	740.1831
ACNthyl	6.50	5.86	3.44	8.64	9.49	5.28	3.84	11.40	36.60	3.6415	119.5532	64.32334
ACNthene	1.86	2.08	2.44	4.82	5.06	3.04	2.55	5.11	10.59	2.614947	124.3195	20.64418
Fl	5.28	4.80	4.54	9.67	10.48	6.87	5.89	8.36	18.86	5.411763	20.83463	17.93514
Phe	9.68	7.60	6.64	21.05	20.29	15.25	6.22	10.36	16.70	6.704481	6.221148	21.68609
Ant	4.95	4.71	4.53	6.20	6.21	5.69	4.49	4.52	7.70	4.451331	8.491858	5.380404
Flu	8.38	6.53	4.58	7.21	6.64	6.56	3.32	6.13	7.98	4.089007	3.227964	14.13078
Pyr	12.58	9.50	5.36	10.04	9.77	8.59	3.63	11.41	37.07	4.873051	4.868486	33.23823
B[a]A	10.50	10.38	9.90	10.80	10.73	11.17	10.10	11.74	11.81	10.65996	16.06448	14.93545
Chry	10.21	10.03	9.64	11.58	11.44	11.99	9.56	9.93	10.08	9.623251	17.11327	21.70048
B[b]F	Nd	8.95	Nd	Nd	Nd	Nd	8.77	8.47	9.08	8.12746	14.67754	8.539048
B[k]F	Nd	8.25	Nd	Nd	Nd	Nd	8.25	8.52	9.16	8.286201	14.19527	8.371875
B[a]P	3.86	3.82	3.53	3.83	3.81	5.01	3.13	3.71	4.03	3.364686	10.92918	6.103313
Pery	3.66	3.33	3.01	3.39	3.26	3.98	3.22	4.32	3.81	4.445491	9.097627	7.477011
InPy	10.75	10.61	10.33	10.20	10.22	10.94	10.12	10.15	14.09	10.25264	15.48201	15.15237
B[ghi]P	4.23	3.90	3.55	3.64	3.58	4.48	3.18	3.20	3.62	3.093624	8.628642	6.54879
DB[a,h]A	8.95	2.30	2.76	2.27	3.81	2.44	0.82	0.82	1.93	0.820538	5.019881	0.802368
C1 Nap	3.49	3.80	4.21	4.71	4.68	45.02	2.29	3.27	3.70	2.020667	35.21238	17.44171
C2 Nap	1.34	1.12	1.37	3.39	3.26	2.20	4.44	12.63	7.66	11.46678	15.21126	48.36027
C1 Phe	10.65	8.13	5.85	35.84	32.36	24.73	5.53	9.06	35.31	6.035092	23.96703	17.62046
C1 Pyr	4.10	3.62	2.72	9.10	9.06	9.38	2.60	2.94	7.09	2.653988	4.504269	8.20591
Retene	1.683569	1.575245	1.58677	2.137288	1.997073	2.025272	1.594122	0	3.062047	0	2.553075	2.204367



Fig. 1: Map of the study area indicating sampling locations

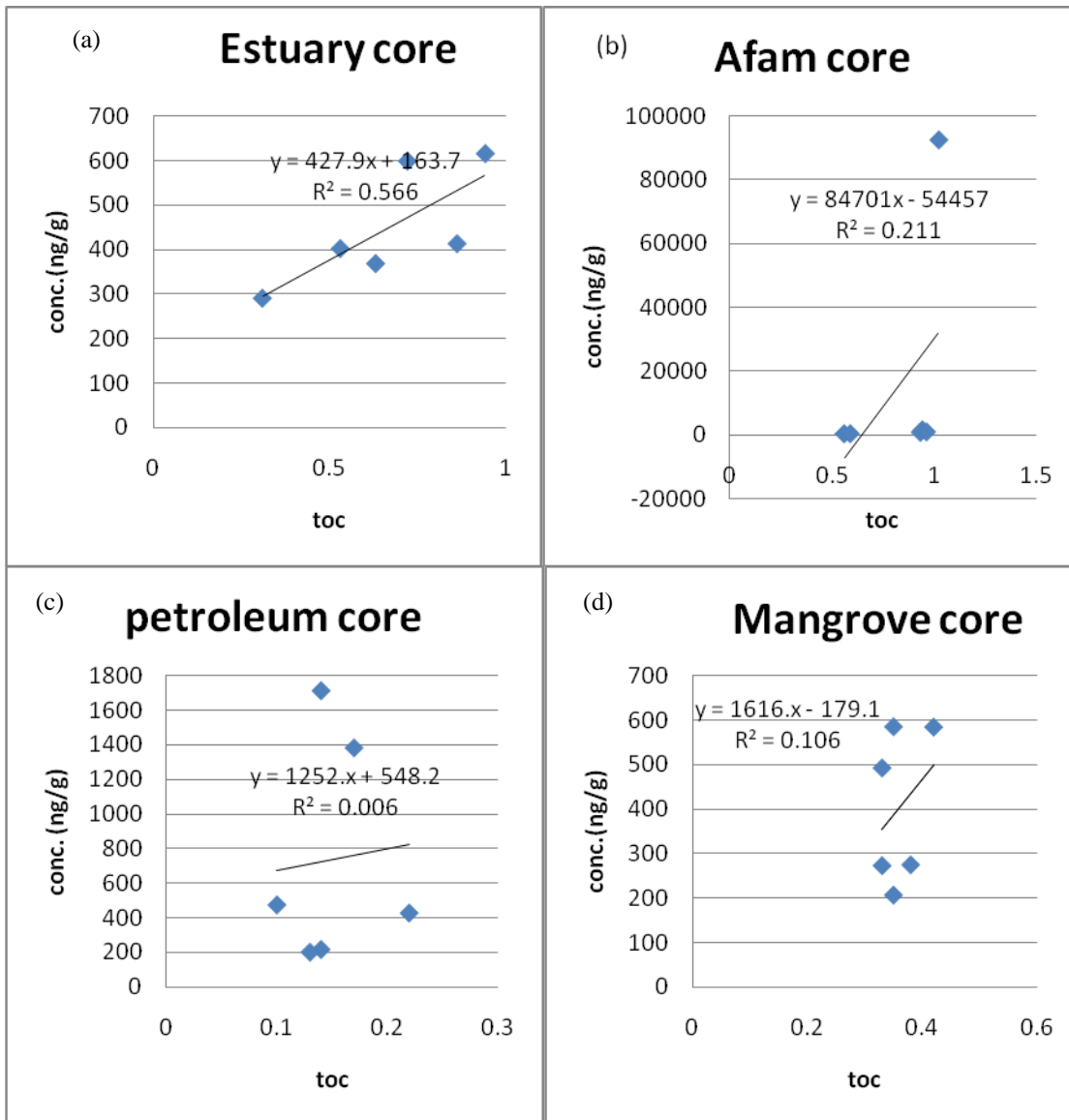


Fig. 2 a, b, c, d: Relationship between TOC and TPAH concentrations for (a) Estuary, (b) Afam, (c) illegal Petroleum refinery and (d) Mangrove sites.

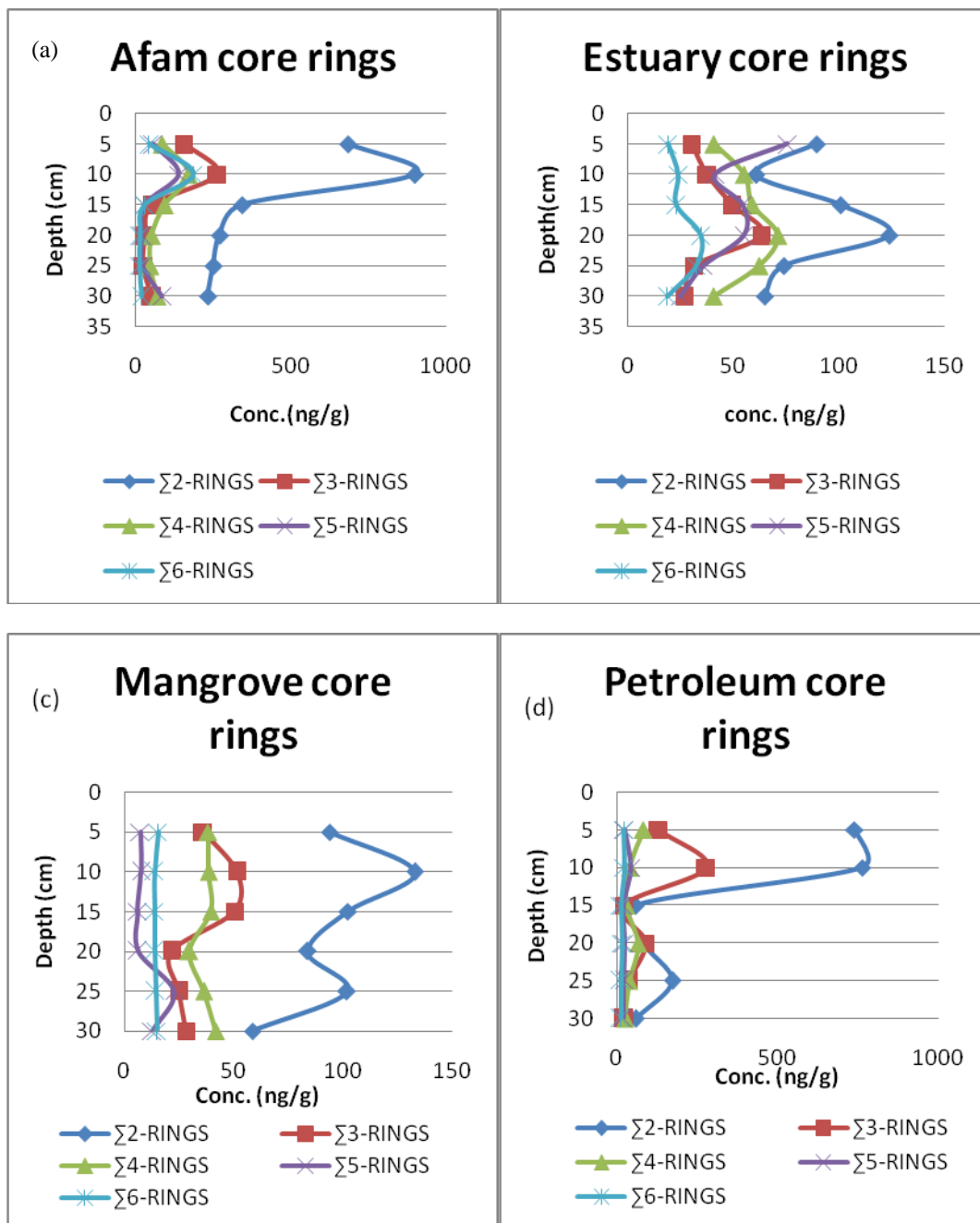


Fig. 3 a, b ,c, d: Vertical distributions of PAHs by number of rings for (a) Afam, (b) Estuary, (c) Mangrove and (d) Illegal petroleum refinery sites.

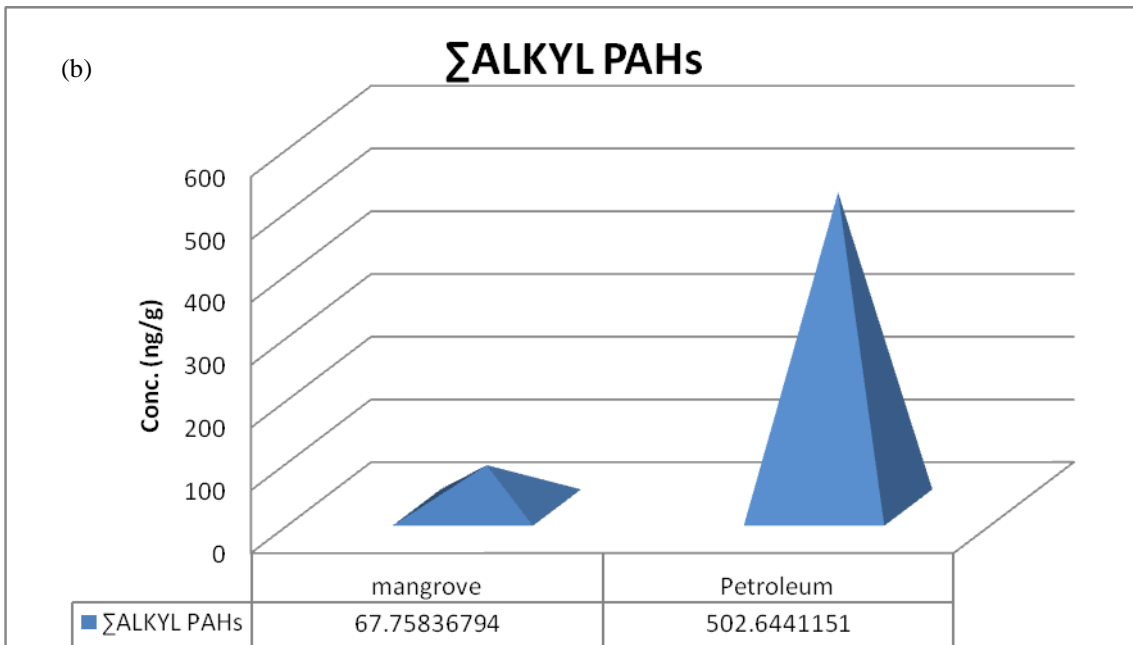
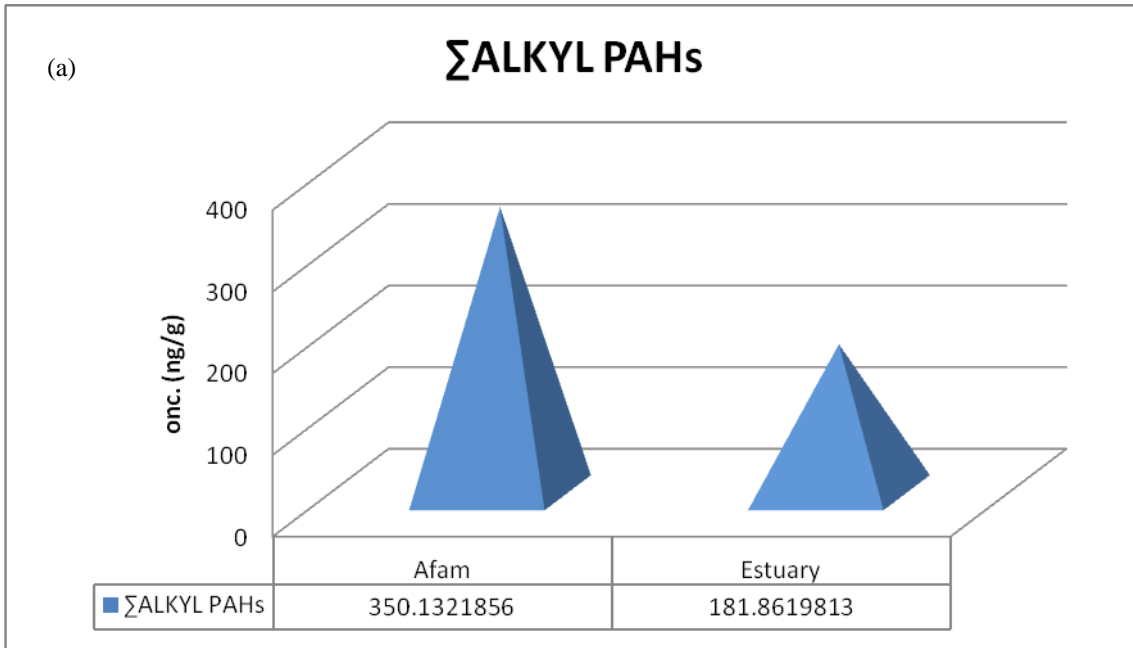


Fig. 4 a, b: Mean concentrations of ΣAlkyl PAHs in top layers of (a) Afam and Estuary sites and (b) Mangrove sites.

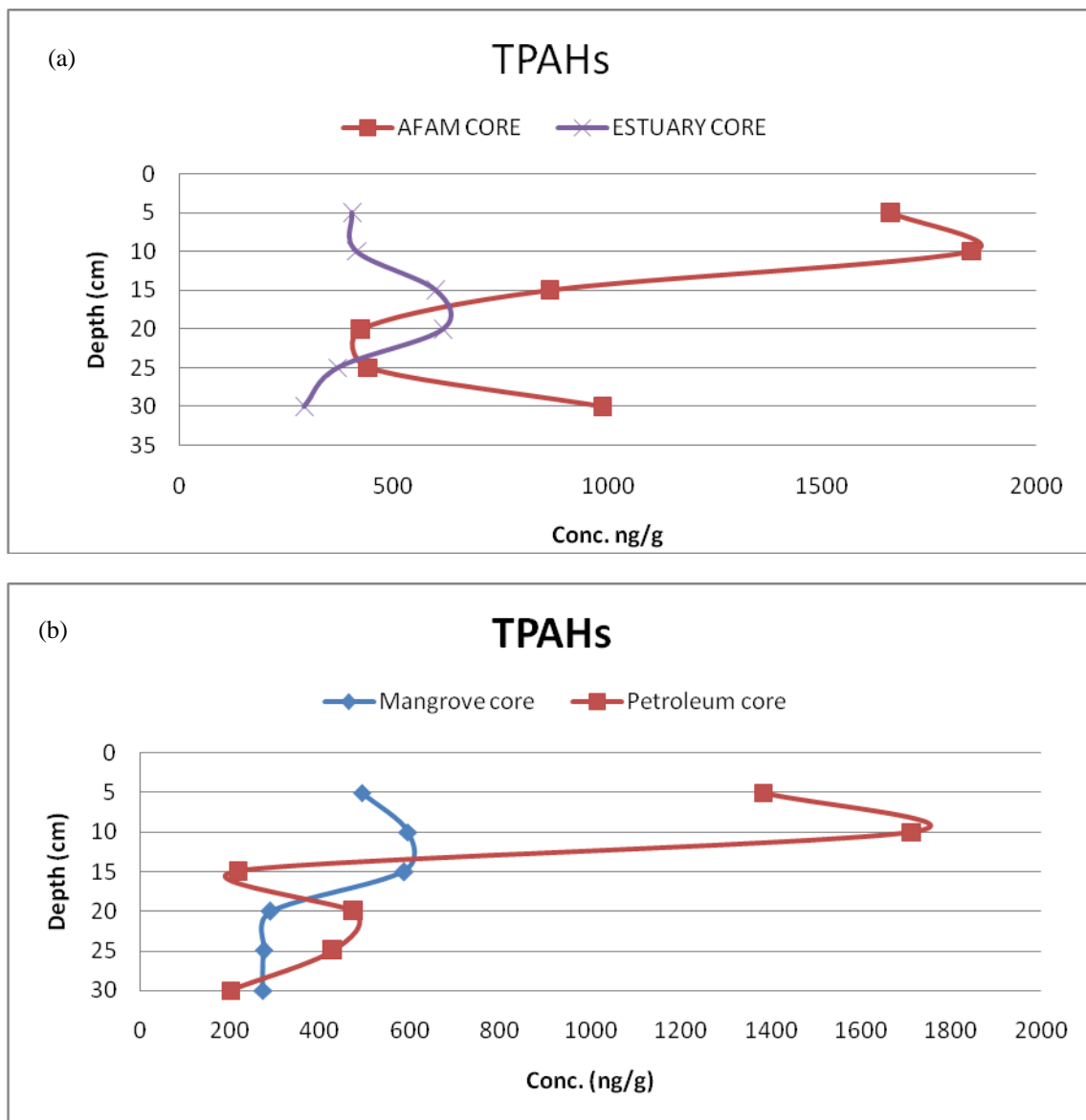


Fig. 5 a, b: Vertical distributions of TPAH in cores from (a) Afam and Estuary, (b) Mangrove and illegal petroleum refinery sites.

Note: AF5 value was normalized by 50 order of magnitude in order to fit into the appropriate scale.

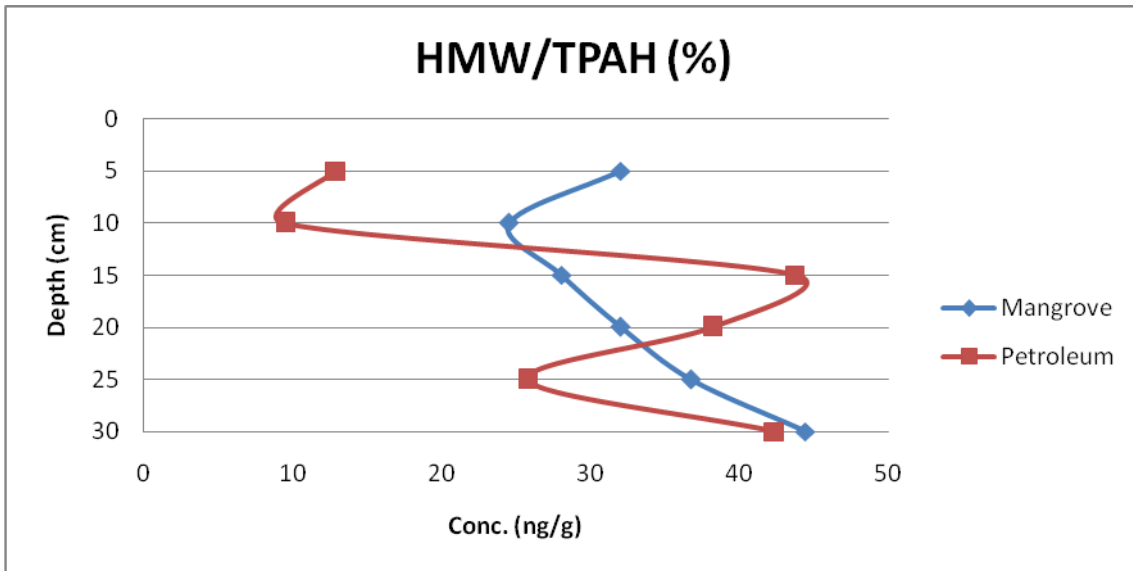
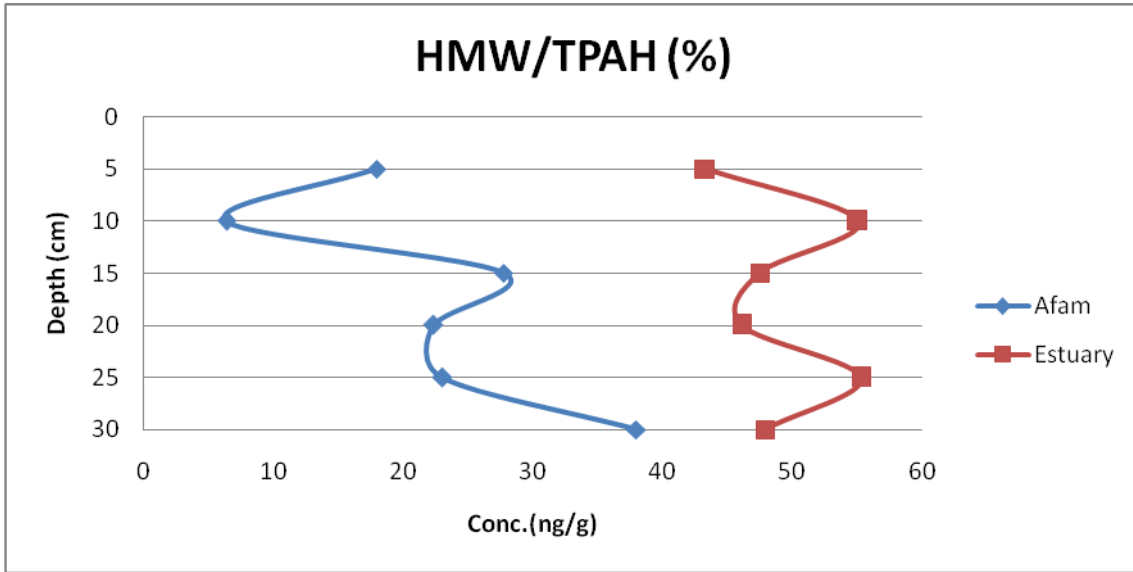


Fig. 6 a, b: Percentage of high molecular weight to TPAHs in (a) Afam and Estuary, (b) Mangrove and illegal Petroleum refinery cores.

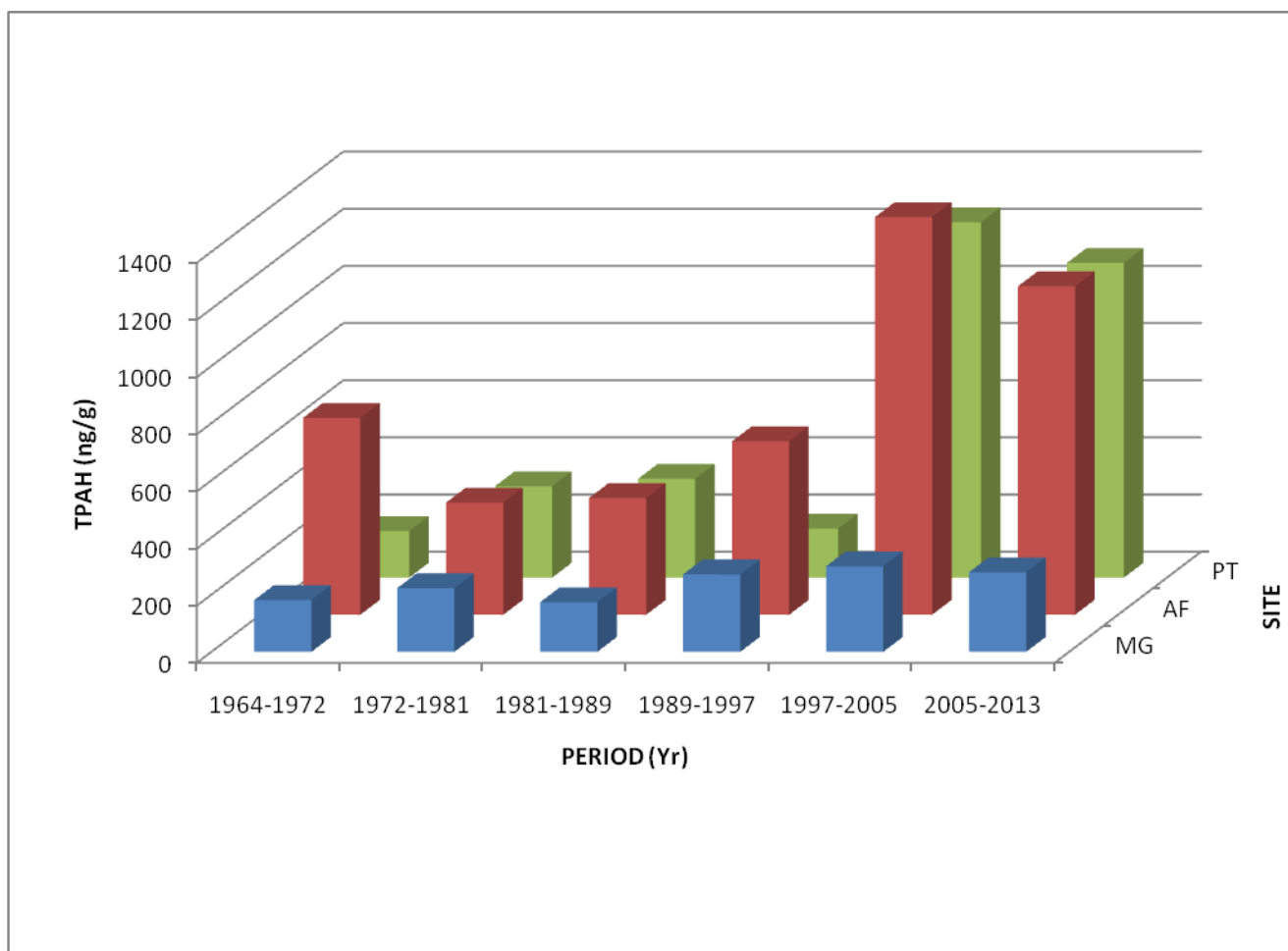


Fig 7: Historical trends of TPAH contamination for the Afam, Mangrove and illegal Petroleum refinery cores.
Note: AF5 value was normalized by 50 orders of magnitude in order to fit into the appropriate scale.

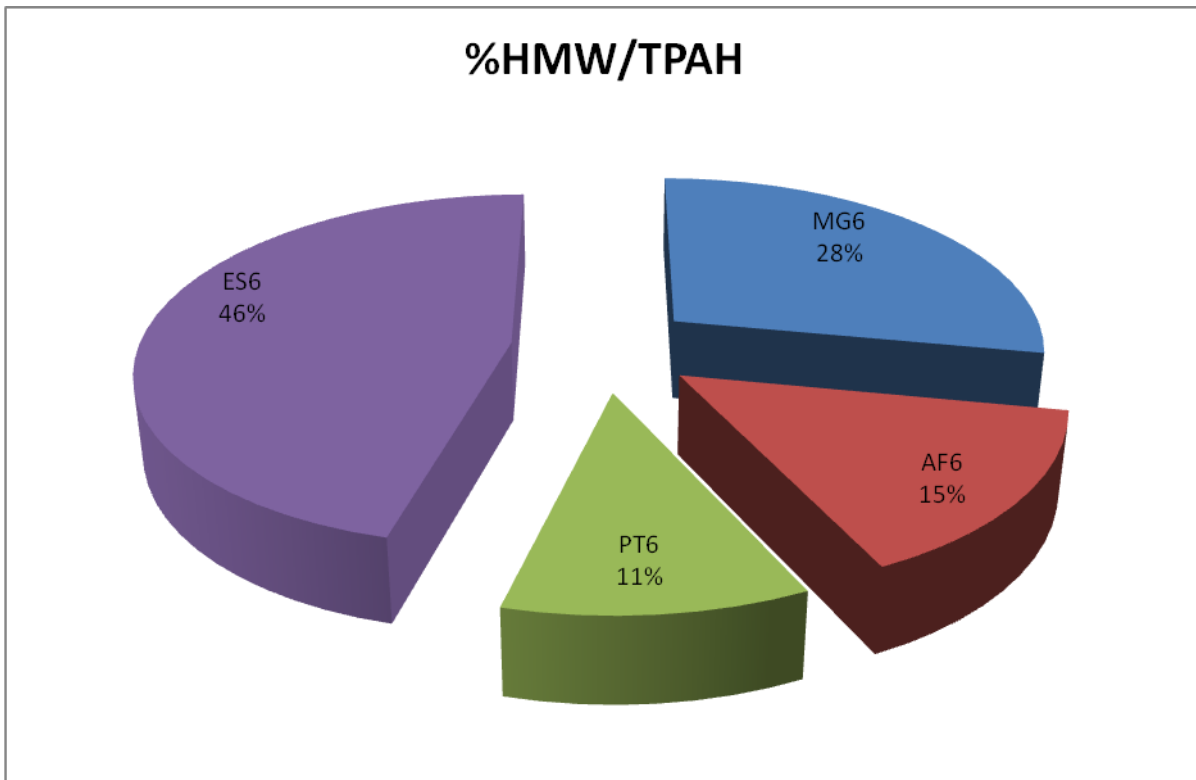


Fig. 8: Percentage of HMW to TPAHs for the top layers of the four sites.

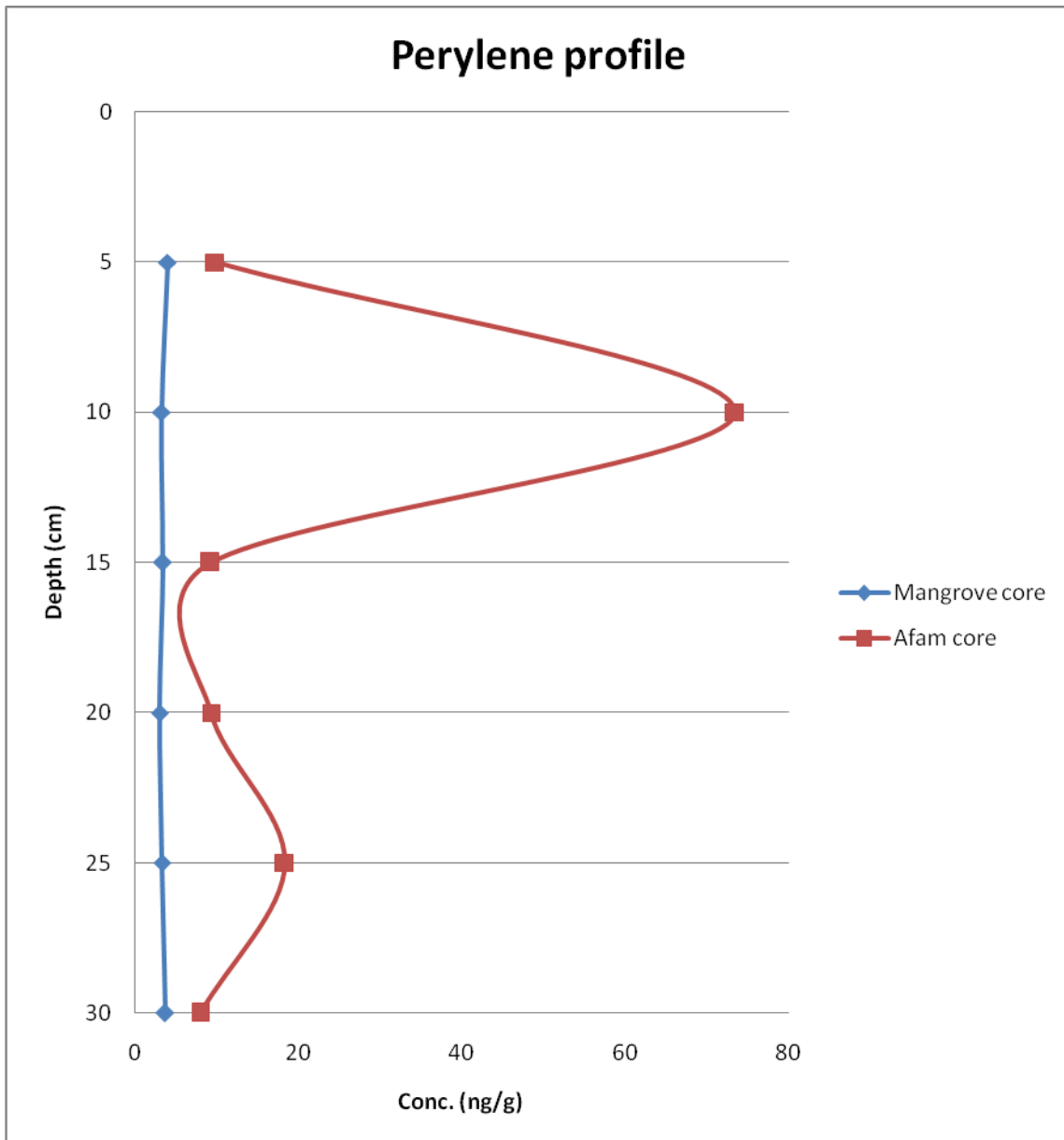


FIG. 9: Concentration-depth profile for Perylene in Mangrove and Afam Sediment Cores.

PROFILE FOR DR INYANG OKON OYO-ITA FCAI

Dr. (Mrs.) Inyang Okon Oyo-ita is a lecturer I with the Department of Pure and Applied Chemistry, University of Calabar, Nigeria. She has her Ph.D degree in Environmental Organic Geochemistry, certificates in SMART notebook software training for SMART BOARD users and a post graduate diploma certificate in advanced study in academic practice from Grenoble, France.

Inyang has developed scientific research collaborative framework that explore research problems through scholarships and creativity with the Environmental and Petroleum Geochemistry research group (EPGRG) university of Calabar, Nigeria, Institute of Environmental Assessment and Water Research Spanish Council of Scientific Research(CSIC) Barcelona, Spain, Laboratory of Biomonitoring of the Environment, Coastal Ecology and Ecotoxicity unit, University of Carthage, Faculty of Science of Bizerte, Zarzouna, Tunisia etc. Dr (Mrs) Inyang Oyo-ita is a member of many professional societies and has also presented quality papers/keynote addresses in National and International conferences. She is an awardee of European Association of Organic Geochemist (EAOG) Travel Scholarship award to Spain, Best session paper and Excellence Keynote address presentation awards at the fifth international conference on Biological, Chemical and Environmental Science (BCES, 2016) in London and a fellow of cooperate administration for a successful combination of research and administrative activities.

SOME OF HER LATEST PUBLICATIONS

- 1 Oyo-Ita, O. E., Oyo-Ita, I. O. and Ugim S. U. (2011). Sources and distribution of polycyclic aromatic hydrocarbons in post-flooded soil profile near Afam power station, SE Niger Delta, Nigeria. *Soil Science and Environmental Management* 7, 35 – 42 (India).
- 2 Oyo-Ita, O..E. Oyo-Ita, I. O. and Ugim, S. U. (2012). Distribution and sources of polycyclic aromatic hydrocarbons and sterols in termite nest, soil and sediment from Great Kwa River, SE. Niger Delta, Nigeria. *Environmental Monitoring and Assessment* 185(2), 1413 – 1426 (Springer Science Publisher, UK).
- 3 Oyo-Ita, O.E. and Oyo-Ita, I.O. (2012). PAHs depositional history in recent core sediments from Ukwabom lake, SE Nigeria. *Environmental Geochemistry and Health* 35, 189 – 199 (Springer Science Publisher, Dordrecht).
- 4 Oyo-ita, O. E. and Oyo-Ita, I.O. (2012). Fatty acids and alcohols distributions and sources in surface sediments of the Imo River, SE. Niger Delta, Nigeria. *Environment and Natural Resources Research* 2, 101 -113 (Canadian Center of Education Publisher, Canada).
- 5 Oyo-ita, O. E, Ekpo, B. O., Oyo-ita, I. O. and Offem, J.O. (2014). Phthalates and other plastic additives in surface sediments of Cross River System, SE, Nigeria; Environmental Implications. *Environment & Pollution*, 3(1), 60-72 (Canadian Center of Education Publisher Canada).
- 6 *Oyo-Ita, O..E. Oyo-Ita, I. O. and Ugim, S. U. (2013). Distribution and sources of polycyclic aromatic hydrocarbons and sterols in termite nest, soil and sediment from Great Kwa River, SE. Niger Delta, Nigeria. *Environmental Progress WWW. environment progress. Org.*
- 7 Oyo-Ita, O..E. Oyo-Ita, I. O. (2015). *Polycyclic aromatic hydrocarbons*. Nova Science Inc. Publisher, New York (USA).
- 8 Dosunmu, M. I., Oyo-Ita, I. O. and Oyo-Ita, O., E., (2016). Risk assessment of human exposure to polycyclic aromatic hydrocarbons via shrimp (*Macrobrachium felicinum*) consumption along the Imo River catchments, SE Nigeria. *Environmental Geochemistry and Health* 38(1), 1-15 (Springer Science Publisher, Dordrecht)
- 9 Oyo-Ita, I. O., Oyo-Ita, O. E., Dosunmu, M. I., Camen Dominquez., Bayona, J. M. and Albaiges, J. (2016). Sources and distribution of petroleum hydrocarbons in recent sediment of the Imo River, SE Nigeria. *Arch. Environmental Contamination & Toxicology* 70 (2), 372-382.
- 10 Oyo-ita, O. E., Oyo-ita, I.O., Sam, E. S., Ekpo, O. I. & Ugim, S. U. (2016). Natural and Anthropogenic biomarkers in recent dated sediment cores from Reforme Lake, SE Nigeria: environmental implications. *Environmental Earth Science* 75 (22), 1-14.